FACULTY OF INFORMATION TECHNOLOGY AND ELECTRICAL ENGINEERING

DEGREE PROGRAMME IN WIRELESS COMMUNICATIONS ENGINEERING

MASTER'S THESIS

THZ RF MEASUREMENT TECHNIQUES

Author	Md Showkat Ali Mollah
Supervisor	Markus Berg
Second Examiner	Risto Vuohtoniemi

June 2021

Mollah Md Showkat Ali. (2021) THZ RF Measurement Techniques. University of Oulu, Faculty of Information Technology and Electrical Engineering, Degree Programme in Wireless Communications Engineering. Master's Thesis, 36 p.

ABSTRACT

In this thesis, literature review on available methods, techniques and procedures for terahertz antenna measurement system and terahertz propagation measurement system are reported. The paper presented the terahertz frequency spectrum allocation by FCC, ITU, ETSI and its application in wireless communication system with advantage in obtaining terabits per second data rates. Terahertz antenna parameters are reported and measurement systems for measurement of these chapters are reviewed.

Literature of three papers on terahertz antenna measurement system with their respective measurement setup, calibration techniques and measurement procedures are reviewed. An automated antenna measurement system is reviewed with stochastic and systematic measurements and has achieved terahertz antenna s-parameter measurements in far field region at frequency range of 220 GHz to 330 GHz. Another measurement system with single port short-open-load (SOL) calibration technique is reviewed. In this measurement of s-parameter of terahertz antenna is carried out, using receiver horn placed on 3 D positioner, which records the AUT 3D radiation pattern. The third paper reviewed, is a reconfigurable terahertz antenna measurement system, with capabilities of working on large bandwidths, with small change in work bench instrumentation. This setup contains the multiplexing stages for terahertz frequency generation. Beam pattern measurements are conducted at 1.37 THz supporting the simulations and the system stability for reconfigurations.

In the later study, terahertz propagation parameters are studied and presented for review of available terahertz propagation measurement systems. Literature review of three papers describing different setup and procedures for terahertz propagation measurement system are reported. The first system with the setup to record path loss in LOS and NLOS links at 260 GHz to 400 GHz is presented. Propagation parameters containing reflections, shadowing is measured. LOS and NLOS channel capacity models are obtained based on data rates in terabits per second for using above 5G wireless communication systems. Another system with office architecture, indoor LOS link, viable for indoor wireless communication applications is reported. Propagation parameters containing power density profile (PDP) are measured and validated for 140 GHz to 220 GHz. A measurement system which reports effect of atmospheric pressure, temperature and humidity is reported in the last. The setup used short, offset-short, load and thru (SOLT) technique for calibration and PDP propagation parameter is measured for 0.5 THz to 0.75 THz.

Terahertz antenna and wave propagation measurement system reviewed in the papers are vital for development of terahertz systems in wireless and mobile communication. Further the study can be extended for measurement of terahertz antennas and wave propagation parameters with models of use in wireless hand-held devices, connected devices, mobile backhaul system and more.

Keywords: Radio frequency, Terahertz, LOS and NLOS links, Antenna measurement, Propagation measurement.

TABLE OF CONTENTS

FOREWORD

This thesis has been carried out as a partial requirement for the completion of the degree towards the Master's degree programme in Wireless Communication Engineering at University of Oulu, Finland, under the supervision of Dr. Markus Berg and Risto Vuohtoniemi.

I would like to thank my supervisors Dr. Markus Berg and Risto Vuohtoniemi for guiding me not only on the theoretical studies but also for the technical support. Their valuable directions, suggestions and comments were required for me to complete the thesis. I would like to thank my parents and wife for their continuous inspirations for my studies. I am also thankful to my friends for their cordial support.

I dedicate this thesis to my parents and wife for their wonderful support throughout my journeys of life and never ending of care.

Oulu, June 11, 2021

Md Showkat Ali Mollah

LIST OF ABBREVIATIONS AND SYMBOLS

2D	2 dimensional
3D	3 dimensional
4K	4000 pixels
8K	8000 pixels
4G	Forth generation
5G	Fifth generation
6G	Sixth generation
7G	Seventh generation
AQI	Air quality indexing
AUT	Antenna under test
CPU	Central processing unit
CMOS	Complementary metal oxide semiconductor
cm	centimetre
dB	decibel
dBi	decibel relative to isotrope
dBm	decibel referenced to milliwatt
DC	Direct current
EHF	Extremely high frequency
EM	Electro magnetic
ETSI	European standard telecom institute
FCC	Federal communications commission
Gbps	Gigabits per second
GHz	Gigahertz
HD	High definition
Hz	Hertz
IEEE	Institute of electrical and electronics engineers
IF	Intermediate frequency
IoT	Internet of things
ITU	International Telecommunication Union
IVTS	Informal value transfer system
KHz	Kilohertz
LO	Local oscillator
LoS	Line of sight
MCU	Microcontroller unit
mm	millimeter
mmwave	millimeter wave
MIMO	Multiple input multiple output
MPEG	Moving picture experts group
NLoS	Non line of sight
PCS	Personal communication system
PDP	Power delay profile
PNA	Performance network analyzer
RF	Radio frequency
Rx	Receiver
SOL	Single port short-open-load
SWR	Standing wave ratio

Tbps	Terabits per second
THF	Tremendously high frequency
THz	Terahertz
Tx	Transmitter
TRX	Transceiver
UE	User equipment
VLC	Visible light communication
VLS	Visible light spectrum
VNA	Vector network analyzer
WLAN	Wireless local area network
YIG	synthetic yttrium iron garnet

D	Directivity
E	Electric field
E_o	Electric field amplitude
G	Antenna gain
G_r	Receiver gain
G_t	Transmitter gain
H	Magnetic field
H_o	Magnetic field amplitude
N	Multiplier multiplication factor
P_r	Received input power
P_t	Transmitted power by the receiver antenna
R	Near field radiation
L	Antenna length
L_r	Received path loss
L_t	Transmitted path loss

λ	Wavelength
ω	Angular frequency
t	Time elapsed
k	Wavenumber
ε_0	Permittivity
ε_r	Relative permittivity of the medium
μ_0	Permeability
μ_r	Relative permeability of the medium

1 INTRODUCTION

The application of THz submillimeter band in the field of wireless communication, internet of things (IoT) [1], [2], intelligent vehicle system [3], indoor short range communication [4], personal communication system [5]. Use of terahertz frequency band over current microwave band from the radio frequency spectrum has immense improvements and application in wireless communication and other fields. 5th generation (5G) and future 6th generation (6G) of telecommunication require wide bandwidth for intensive MIMO, terahertz frequencies has wide bandwidth which fulfils these requirements [6], [7], [8], [9]. High resolution imaging [12], [13], [14], [15], spectroscopy for biomedical and pharmaceutical [10], [11], wireless sensor network and other higher bandwidth and data rate applications has raised the need to further explore the THz frequency band system.

With rapid development in integration, power optimization and high data rate applications, coming in the future is expecting low cost, low power handheld user equipment (UE) compatible with wireless communication network with throughput in terabits per second (tbps) [17].

The promising THz scope in majority of fields, as a replacement over current GHz band. This has opened roads for research in THz system inclusive of THz antenna, wave propagation, channel modelling, RF band acquisition, radiation detection, terahertz sources and THz applications. In the current thesis, THz measurement technique are studied and literature review of the published work in the field is analyzed and presented with their respective measurement system, prototype, proof of concept, techniques and results. Further the study is extended for commercial viability checks of the presented methods and techniques, based on this future work scope is proposed [16].

1.1 THz band Methods and Techniques

The current frequency channel bandwidth is flooded due to rapid increase in highly efficient, high resolution and high precision applications. These requirements demand more throughputs or data. The throughput requirements in wireless communication system are drastically increasing and are exceeding the throughput limits of wired and optical fiber [2]. Some of the developed applications are requesting more than 100 Gbps throughputs. The traditional techniques for wireless sensing, imaging, spectroscopy, material science, communication and more, are seeking more bandwidth. The huge spectrum and channel bandwidth of terahertz frequencies with mmwave and THF band has complete scope to develop new methods to overcome spectrum issues over the traditional technologies [2]. The current RF measurement methods shows complexity for THz frequencies band system. Equipment like spectrum analyzer and similar devices are precise for frequencies under few THz frequency range, devices like vector network analyzer (VNA) are deployed using different techniques for THz frequency band system [2]. In this thesis, we will do detail study of the existing methods and techniques in THz frequency band system for different applications and their limitations. Further we will propose future work scope for improvement and enhancement of the presented terahertz measurement technique in THz frequency band system [2].

2 THZ FREQUENCY RANGE AND APPLICATION

Terahertz frequency range between 300 GHz to 3 THz from the microwave region to the infrared frequency region. THz frequency also lies in the visible light spectrum (VLS), with frequency range between 430 THz to 730 THz [17]. And this range covers between the millimeter wave EHF and submillimeter wave THF band. Wireless communication using this VLS spectrum named as visible light communication (VLC) is a proven model reported in the future. Many researchers have been conducted and commercial test equipments are made for VLC [22]. VLS spectrum has certain limitation to be used in majority of THz frequency band applications. These limits are the spectrum utilization between millimeter and submillimeter waves in THz frequency band system. The wideband THz frequency band system has potential applications with parallel utilization of the wide channel bandwidth in different wireless communication technique like high speed WLAN. IEEE has developed the standard, high data rate personal communication, internet of things, high speed cloud computing, high resolution image sensing, smart cities with smart transportation system, secured communication. In the coming 5G and future 6G and above telecom generations, THz is replacing optical fiber backhaul with THz line of sight (LOS) links. And in the same generation user equipment and other smart telecom devices are scaled to nanotechnology fabrication with use of short wavelength on-chip antenna and transceiver as well as non line of sight (NLOS) communications [23].

2.1 THz Frequency Spectrum

The 4th generation of mobile communication (4G) operating under 6 GHz is a big success towards its set commercial data rate limits. Further the spectrum shortage in 4G is resolved in the 5th generation (5G) with successful benchmarked testing across the world. While development and standardization phase of 5G data rates, data throughput demand raised above 5G standardized data rates due to increase in wireless traffic. Data enrich applications, Internet of things (IoT), optical to radio frequency convergence and many more as stated here in the thesis. This has raised the bandwidth requirements and spectrum needs for spectrum above 5G [17]. In the running spectrum, terahertz frequency range under tremendously high frequency band (THF), with wavelength of 10 mm to 1 mm [18] is considered as the last piece of RF spectrum viable for wireless applications [19]. The figure 1 illustrates the presence of terahertz frequency band viable for wireless applications up to 0.1 mm in wavelength. Millimeter wave lies under extremely high frequency (EHF) band, ranging from 300 GHz to 3 THz frequency range, under 10 mm to 0.1 mm wavelength exhibits data rate above 100 Gbps [17], [18]. Although visible light has frequency range in terahertz but is out of THF band. Visible light communication (VLC) has also been experimented with data rate in tbps and is under research for commercial use [22].

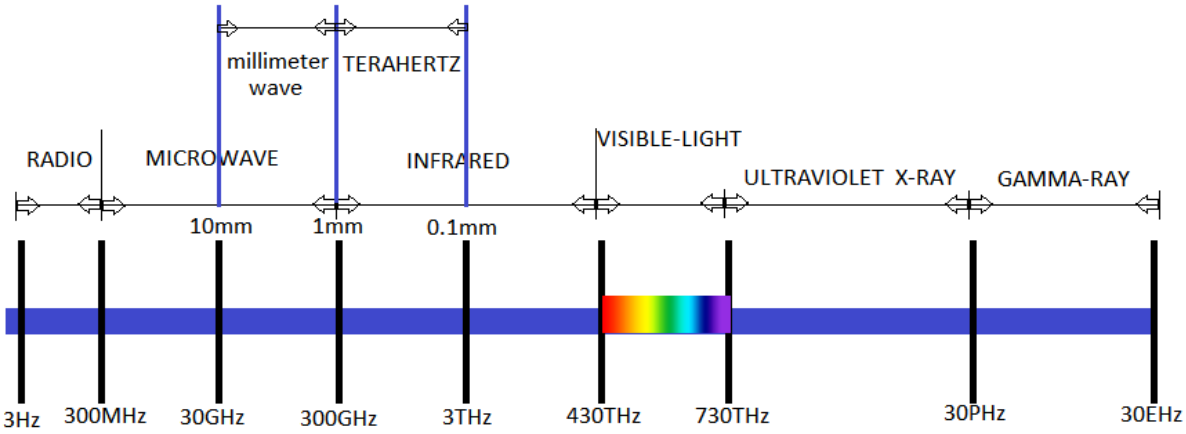

Figure 1. Radio frequency spectrum [17], [18].

2.1.1 THz Frequency Channel

The Federal Communications Commission (FCC) and other telecom bodies were in discussion and seeking remarks for frequency allocation above 95 GHz [17], [19], [25]. Table 1 shows all the channels available under EHF band THz frequency [25]. The frequency channel allocation in the millimeter wave region have been done by FCC in year 2018 [17], [20], [25] and a rulebook is made for spectrum between 95 GHz to 275 GHz for government and non-government use. Table 1 below demonstrates the whole table of frequency channels and their respective bandwidths [20], [17], [25]. In year 2019, the telecom bodies inclusive of FCC, International Telecom Union (ITU) and European Standard Telecom Institute (ETSI) has provided 21.2 GHz of unlicensed spectrum for use in USA [17], [25]. Ranging between 95 GHz to 275 GHz and has opened licensing up to 3 THz for research and experimental purpose [25]. In 2017, the Institute of Electrical and Electronics Engineering (IEEE) has proposed 8 different bandwidth channels, for wireless communication system, under frequency range of 252 GHz to 325 GHz. The bandwidth ranges from 2.16 GHz to 69.12 GHz, with data rates approaching 100 Gbps. The work is carried out under IEEE standard 802.15.3d in 2017. With the utilization of the data rate IEEE proposed a new standard 802.15.3e for file transfer of 4K high definition (HD) MPEG in less than 250 ms [20], [23], [25].

Table 1. FCC standardized terahertz frequency channels [20], [25].

Frequency Band (GHz)	Channel Bandwidth (GHz)
95-100	5
100-102	2
102-105	3
105-109.5	4.5
109.5-111.8	2.3
111.8-114.25	2.45
114.25-116	1.75
116-122.25	6.25
122.25-123	0.75
123-130	7
130-134	4
134-136	2
136-141	5
141-148.5	7.5
148.5-151	3
151.5-155	4
155.5-158	3
158.5-164	5.5
164-167	3
167-174.5	7.5
174.5-174.8	0.3
174.8-182	7.2
182-185	3
185-190	5
190-191.8	1.8
191.8-200	8.2
200-209	9
209-217	8
217-226	9
226-231.5	5.5
231.5-232	0.5
232-235	3
235-238	3
238-240	2
240-241	1
241-248	7
248-250	2
250-252	2
252-265	13
265-275	10

FCC has allocated unlicensed frequency channels of total bandwidth of 21.2 GHz in mmwave EHF band THz frequency. Table 2 provides the detail of all the unlicensed frequency channels in THz frequency range [20], [25].

Table 2. FCC allocated unlicensed THz channels [17], [19], [20], [25].

Frequency band (GHz)	Channel bandwidth (GHz)
116-123	7
174.8-182	7.2
185-190	5
244-246	2
Total	21.2

2.2 Terahertz Applications

Terahertz frequency spectrum is used in wide areas, all tradition in present microwave wireless RF applications has equally deployed in THz frequency band system with enhanced bandwidth. This has offered space for more data-traffic, applications, extremely higher data for higher order applications, great scope for wireless backhaul [20], [25], [26].

2.2.1 Terahertz Wireless Communication

Augment reality, 8K and above resolution, optical to RF convergence for backhaul and much more are the key application of THz frequency bandwidth over traditional spectrum. The advanced 5G, upcoming 6G and beyond generations of wireless telecommunication will deploy THz spectrum and nano-scale hardware user equipment UE [20], [25], [26].

Nano-scale hardware with embedded on-chip CPU, MCU, antenna is made possible due to small CMOS packages with antenna dimensions of few millimeter wavelengths of THz frequencies. The future UE is expected to be of whole cloud memory and with use of higher data rates in tbps all applications will run in real time [20], [25], [26].

Terahertz comparison and application over current spectrum is presented in the Table 3 below:

Table 3. Terahertz applications in wireless communication [20], [25], [26].

Wireless communication			
Services	Spectrum	Present data rates	THz proposed bandwidth
Telecommunication	under 5G standard with present auction 24 GHz and 27 GHz bands with total bandwidth of 15.5 GHz	<10 Gbps	low THz range from 95 GHz to 275 GHz with bandwidth of 180 GHz
Personal Communication System (PCS)	current allocation 6 GHz band with bandwidth 1.2 GHz	1.73 Gbps	current allocation 95 GHz to 275 GHz band with bandwidth 21.2 GHz
Internet of Thing (IoT)	current allocation 6 GHz band with bandwidth 1.2 GHz	1.73 Gbps	current allocation 95 to 275 GHz band with bandwidth 21.2 GHz
Intelligent Vehicle Transportation system (IVTS)	current allocation 6 GHz band with bandwidth 1.2 GHz	1.73 Gbps	current allocation 95 GHz to 275 GHz band with bandwidth 21.2 GHz

2.2.2 THz Imaging

Imaging comprises of satellite imaging, radar, and security. The traditional techniques utilizing current spectrum are under boundaries of limited resolution, limited pixel density, bandwidth and visible light dependency. Terahertz frequencies overcome these limitations [14], [15].

Traditional image detection with use of infrared and visible light is temperature and weather condition sensitive. Replacing infrared or visible light with terahertz radiation makes it possible to achieve high resolution detection, unaffected by change in ambient conditions and weather. Terahertz wide bandwidth provides high resolution, good pixel density imaging in satellite imaging [14], [15].

Combination of current radar system and THz detection will lead to high resolution and precision detection in long range and all in weather conditions. The high precision imaging provides advantage in security application over traditional system [14], [15].

2.2.3 THz Sensing

Many sensing applications under THz frequencies are widely studied, comprising of air quality indexing (AQI), gesture detection, medical equipment sensors and more [16]. With wide channel bandwidth, transmission of multiple sensing signals under set protocols can recover 3D structure in real time [16]. Figure 2 below shows the sensing equipment setup.

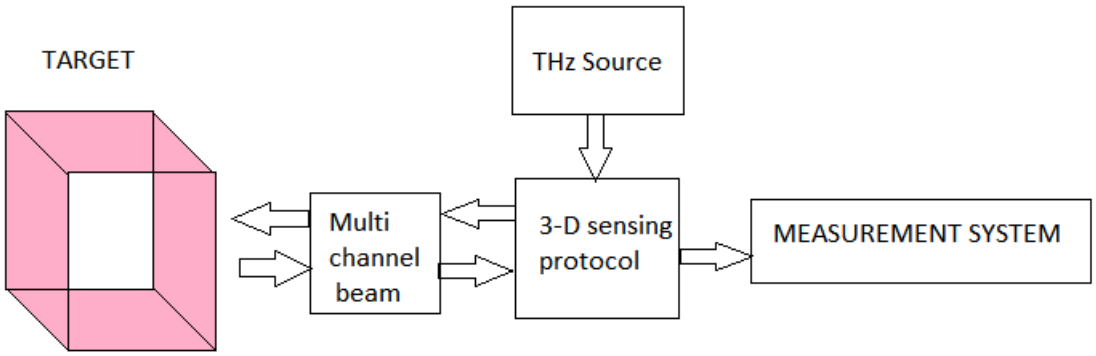

Figure 2. Terahertz sensing setup for 3D structure [16].

3 THZ ANTENNA PARAMETERS

Electromagnetic wave transmission and detection in the free space is carried out by the basic radio frequency element named as antenna. Antenna design, selection, specification are core parts for electing antenna for certain specified frequency band [27], [30]. As THz frequency is ranging from microwave to photonic level, antenna design approach is the major field of research in THz (EHF and THF) frequency band. Carrying out telecommunication under terahertz frequency band is future potential approach for beyond 5G networks [28]. Antenna parameters inclusive of radiation pattern, gain, s-parameters, SWR, transmission loses are among the major design parameters considered for telecommunication and other terahertz applications [28], [30]. This chapter contains the detailed understanding of the important antenna parameters and their utilization in designing of the antenna under terahertz frequency band for different applications.

3.1 Terahertz Antenna

Antenna is a device which converts the high frequency electrical signals guided by the waveguide or a transmission line into radiation in form of electromagnetic wave in all direction or in dedicated direction in free space [27]. The antenna reveres the conversion of electromagnetic wave coming across, into high frequency electrical signals and acts as receiver [27]. The terahertz frequency band antennas experience small size and high data rates, due to shorter wavelength and wide bandwidth. The shorter wavelength causes high loses and low fabrication precision in the THz antenna design [29], [30].

3.1.1 Antenna Radiation Pattern

The radiation pattern of an antenna is the 3 dimensional or 2 dimensional representation of the radiations emitted by the antenna in the certain region [30]. The radiation pattern region is the region beyond the near field radiation region of the antenna. Near field radiations are in the fresnel region with radius equivalent to the product of antenna length and inverse of wavelength [27], [30]. Beyond near field is the far field region or fraunhofer region [27], [30]. The radius of the near field as expressed R is

$$R = \frac{2L^2}{\lambda}, \tag{1}$$

where L is the antenna length, and λ is the wavelength [30].

The intensity of the radiations forming the radiation pattern is measured in units of watts per unit solid angle and is product of power-density and square of the distance at which power is measured [27], [30].

3.1.2 Antenna Beamwidth

The radiation pattern of an isotropic antenna is measured in 3 dimensional spaces and is plotted using coordinates of the radiated energy. The radiated energy has pair of identical maxima on opposite side; maxima are points where radiation intensity is maximum and is constant. The angular separation between these maxima is considered as the antenna beamwidth. Beamwidth is also stated as antenna aperture from where potential radiation power is radiated [30].

3.1.3 Antenna Directivity

Directivity of an antenna is a dimension less measurement. The directivity of the antenna in a given direction is the ratio of radiation intensity in the direction and mean of radiation intensity in all directions or radiation intensity of an isotropic antenna [29], [30].

Directivity can be presented with its unit in dBi by taking its logarithmic value as presented in the below equation [29], [30].

$$D[dBi] = 10\log D, \tag{2}$$

where D is the directivity of an antenna [30].

3.1.4 Antenna Efficiency and Gain

The antenna radiation efficiency or antenna efficiency is the ratio of effective power radiated by the antenna to the power accepted by the antenna. The power radiated by the antenna is less than the input power feed by the transmission line to the antenna, due to presence of antenna loses. These loses effect the overall performance of the antenna and the parameter defined to study the performance of the antenna is antenna efficiency [29], [30].

The reflection loses at the input terminal of the antenna are due to impedance mismatch between the source as transmission line impedance and the load as antenna input impedance. The ideal antenna has perfect impedance matching and maximum power is transferred between the source and the antenna without loses [29], [30].

Antenna gain measures the performance of the antenna in terms of efficiency and directivity. When the direction is not specific, gain is taken in the direction of maximum radiation. Antenna gain is a presented in dBi by taking logarithmic value of *G*. Antenna gain parameter is equally applicable to antenna in receiving mode based on reciprocity theorem [29], [30].

$$G[dBi] = 10\log G, \tag{3}$$

where *G* is the antenna gain [30].

3.1.5 Antenna Bandwidth

The antenna performance parameter inclusive of gain, radiation efficiency, beamwidth, radiation pattern, directivity has achieved to an acceptable optimized value at a certain frequency range. With their maximum optimized values at the centre frequency of the frequency range, this frequency range is measured as the bandwidth of the antenna and the centre

frequency is measured as the resonance frequency of the antenna [29], [31]. Antenna bandwidth parameter is equally applicable to antenna in receiving mode based on reciprocity theorem [30].

The measure of antenna bandwidth defines the operational frequency range of the antenna and has three components as lower frequency, centre, or resonance frequency and upper. Broadband antenna has higher bandwidth in comparison while the narrowband antenna has very small bandwidth [30].

4 THZ PROPAGATION PARAMETERS

Radio wave propagation or RF propagation is an important study for understanding the behaviour of different frequencies while they propagate from different medium over short to long distance. RF frequencies in the THz region are impacted by the atmospheric gases like oxygen and presence of water vapours. During propagation, oxygen and other gases and vapours content in air causes huge attenuation to the radio waves. The attenuation increases gradually with increase in frequency. The attenuation study is carried out by FCC and shows high spikes in attenuation over frequencies 60 GHz, 120 GHz and 183 GHz [19], [25], [27].

The high attenuation limits the propagation properties of EHF and THF band (frequencies under THz band), to short distance communication. Water in any form, vapor, droplets, fog drastically effect the propagation of THz waves and the impact increases with increase in frequency, the study was done in Shanghai University and originally reported in [21], the study shows the change in standard deviation corresponding to strong and weak air turbulence under different temperature and relative humidity levels. Stronger the air turbulence higher the difference in simulated and experimental results, the attenuation increases with increase in frequency. The results are conducted from 0.1 THz to 0.9 THz [21], [27].

In this chapter the electromagnetic wave propagation parameters are introduced to study the attenuation impact on terahertz frequency signals.

4.1 Radio Wave Propagation Mechanism

Electromagnetic wave propagating characteristics and parameters are studied with its propagation through different medium, consists of lossless media, lossy media, rough surface and diffracted edges [27].

4.1.1 Plane wave in lossless medium

Electromagnetic wave propagating through a free space or lossless medium comprises of sum of multiple plane waves propagating in the direction of propagation or pointing vector [27].

$$E = E_0 \cos(\omega t - kz)\hat{x} \tag{4}$$

$$H = H_0 \cos(\omega t - kz)\hat{x} \tag{5}$$

Maxwell's curl equation, equate the plane wave with its associated electric field E and magnetic field H and free space properties permittivity and permeability. The equations are represented as E_0 is the electric field amplitude, H_0 is the magnetic field amplitude, ω is the angular frequency, t is the time elapsed, k is the wavenumber and z is the distance along the z-axis [27].

4.1.2 Plane wave in lossy medium

In the lossless media, the medium characteristics permittivity and permeability changes according to the medium properties. The values of relative permittivity and permeability are taken as 1 in case of propagation through free space or lossless media [27], [30].

$$\varepsilon = \varepsilon_0 \varepsilon_r \tag{6}$$

$$\mu = \mu_0 \mu_r \tag{7}$$

The free space permittivity and permeability are presented by ε_0 and μ_0; where ε_r is the relative permittivity of the medium and μ_r is the relative permeability of the medium [27], [30].

4.1.3 Plane wave on rough surface

Plane wave incident on the smooth surface media boundary possess specular reflection. With incidence of plane wave on progressively rough surface media boundary, reflected wave get scattered from multiple position of the rough surface and increases the scattered energy. This reduces the specular energy. Scattering is the function of angle of incidence, surface roughness and wavelength [27].

4.1.4 Plane wave in shadow region

Huygen's principle is used to define the wave propagation in the shadow region of the completely conductive obstruction. The transmission of incident wave in the shadow region happens due to diffraction; the energy in the diffracted wave in the shadow region is reduced due to absorption by the obstruction [27].

In wireless communication the radio waves are diffracted by all kind of obstructions, including obstructions other than knife edge. The study involves consideration of shape and material of these obstructions to study the diffraction effect [27].

4.2 Radio Channel Modelling

In wireless communication system, the propagation of radio wave from the transmitting antenna to the receiving antenna is modelled based on propagation characteristics and antenna parameters. The terahertz wireless communication channel is modelled for path loss, shadowing and fading [27].

4.2.1 Path Loss

The wave propagation from the transmitted antenna to the receiving antenna experience interaction with the loss elements and objects between the transmission path causing fading, shadowing and other loses [27].

$$P_R = \frac{P_T G_T G_R}{L_T L L_R}, \tag{8}$$

where path loss calculation are made, considering the loss L and gain G elements in the system and is express in terms of received input power P_R and P_T presents the transmitted power by the receiver antenna [27], [30].

4.2.2 Shadowing

The signal power or strength varies with type of clutter, this phenomenon is known as shadowing also termed as slow fading. Shadowing is considered over large distance points in the clutter. Shadowing transforms the pathloss prediction model which ensures fixed predictable values, into statistical expressions which predicts the coverage and capacity values of the communication channel [27], [30].

4.2.3 Fading

The phenomenon by which signal strength varies rapidly over short distances is termed as fast fading. Fast fading effects are modelled using the statistical approach. Fading occurs due to presence of multipath signals arrives at the receiver from line of sight (LOS) path and it is also possible from non line of sight (NLOS) path from the source. The multipath signal propagation arrives due to scattered waves from the obstacles between the transmitter and the receiver [27], [30].

5 TERAHERTZ ANTENNA MEASUREMENT SYSTEMS

In the wireless communication system, antenna is the first element at the receiving end circuitry and the last element at the transmitter end circuitry. Antenna provides the wireless interface between the transmitter and receiver over different frequency spectrum. Antenna parameters are inclusive of radiation pattern, gain, directivity, bandwidth, beamwidth, efficiency. Antenna structure and type are characterized based on the wireless communication frequency spectrum in utilization. Antenna captures or radiates the electromagnetic waves (EM) of frequencies, under the frequency band in use, over free space and other medium [31]. Waveguide, transmission line and feeders are used to guide the waves to and from the antenna for emission and detection. In transmitters, waves with different frequencies are generated by source connected to the antenna via waveguide, transmission line or feeders; receiver has the same geometry with detector replaced with source to detect the signals. In terahertz frequency band system, the components at transmitter and receiver are replaced with modelled high frequency components, developed and tested under terahertz frequency band [31]. The material characteristics and component structures, used in design of terahertz antenna, waveguide and other components are very different in comparison to traditional megahertz components. This study will cover the roadmap of terahertz antennas design and characteristics, and the associated measurement techniques [31].

5.1 Spherical Positioning System

Measurement system design, placement and instrumentation in mmwave consists of custom mechanical structure designed as positioning system in the measurement system has its x-y positioning in horizontal direction and z axis towards the roof of the room and is spherical in shape. Complete system is placed on air suspended optical table to avoid degradation in mmwave measurements during vibration. The remaining room is treated with vibrational decoupling, which allows easy shift and removal of standard optical and mmwave components on the optical table. An industrial rack sizing 19 inches is stacked near the system, with control unit, drive unit of the positioning system, VNA, local oscillator (LO), DC power supply, personal computer, RF coaxial cables, DC cables and vacuum tubes [32].

Receiver positioning and placement in the measurement setup consists of rectangular frame of plastic wood composite material is used to guide cable on the optical table. The positioning system is sitting inside the frame on the optical table, with placement of receiver on it, which provides degree of movement in azimuth and elevation. RF and DC cable are mounted on the frame and are aligned coaxially in z axis to avoid bending of cable during azimuth moments. For moments in elevation RF cables are supported with loop [32].

Frequency converters are positioned in 3 dimensional alignment using two cartesian motor-driven manipulators. On-chip antenna and open-ended rectangular waveguide as AUT, has central positioning on the frame, with manual placement in x-y plane. Laser beam position marking is used in the setup for accurate alignments in manual placements. Camera based microscope is used for accuracy in wafer probing in on-chip antenna measurements. The microscope is mounted on another cartesian motor driven manipulator. Another receiving frequency converter is mounted via a hook for free elevation moments during far field measurements. Two versions of hook with different material type are used, one with polycarbonate another with cladded aluminium [32].

The setup involves measurement capabilities in transmission and reflections using on wafer probe feed and rectangular waveguide. One of the mmwave frequency converters mounted on the optical table is used as TRX port in the setup and is used without receiver in S_{11} parameter measurements for both on chip and rectangular waveguide. Another frequency converter mounted on the optical table is used as receiver for S_{11} and S_{21} measurements. The receiving frequency converter hooked on the spherical positioning system, is used for S_{11} and S_{21} far-field measurements. The measurements involve input s-parameters (S_{11}), recorded without changes in spherical coordinates using microscope adjustments in elevation, far field s-parameters (S_{11} and S_{21}) recorded with elevation adjustment using hook adjustments in steps on spherical positioning system. The complete method is used to obtain different parameters with flexibility in positioning of AUT, transmission port and receivers, using microscope and radar for higher accuracy [32].

The setup experience reflections during far field measurements and creates errors in results. To overcome this effect, the fabricated material of the positioning system is cladded with mmwave absorbers are fabricated with low loss dielectric material. The system has self characterization methods for reflection characterization using available devices and materials. Reflection contributions are studied with time-domain analysis of S_{11} parameters, the setup contains an open-ended waveguide as AUT, positioned at z=0 plane, surrounded by a mmwave absorber collar and the VNA for measuring input reflection coefficient S_{11}. The AUT moves around the rectangular grid to record reading at different positions. The reflections spikes and peaks are studied under time domain analysis and disturbance observed are very week. The other cause of reflections are the metal parts of frequency converters working as receivers, cartesian motors, and reflections due to RF, DC and optical cables. Reflections can be further supressed with use of cladding on receivers to improve the precision of the measurement method [32].

Another parameter of interest in the measurement method is to carry out repeated measurements, evaluated on the basis of phase uncertainties. Phase changes are subjected to probe displacement and radial trace deviation. The measurement setup contains AUT positioned in the origin as transmitting antenna and frequency converter hooked to spherical positioning system as receiver. Repeated measurements are done with polycarbonate and aluminium hooks and expressed in standard deviation model with change in elevation at fixed azimuth. Aluminium hook has provided better phase stability and has reduced radial errors in spherical positioning moments of receiver. The repeated measurements are shown negligible effect on amplitude measurements [32].

Measurement system validation using open ended waveguide as AUT, gain, radiation pattern 2 D and 3 D measurements with AUT positioned at origin. Realized gain measurements in dBi, are recorded, using VNA in 2 D across full frequency range of 220 GHz to 320 GHz and are in good agreement with the simulation results. 2 D radiation pattern are constructed using measurements in E-plane (x-z plane) and H-plane (y-z plane) and 3 D radiation pattern are constructed using measurements made in azimuth and elevation traces twice at different receiver orientation. both 2 D and 3 D plots at 220 GHz and 330 GHz are in good agreement with the simulation results and supports the measurement system with high accuracy [32].

5.2 Far Field Antenna System

The block diagram in the figure 3 describes the schematic of the measurement setup and describes the connections, component placements and instrumentation. The mmwave frequency

extender feeding the AUT via coaxial probe or waveguide is connected to the mmwave frequency controller which feed it with VNA RF signals and LO and IF signals [33]. At the frequency extender stage, LO signals are multiplied using frequency multipliers and generates mmwave in terahertz frequency band. The signals are guided with the selected waveguide or coaxial line and feed the AUT to radiate in space. AUT impedance measurements are obtained with reflection measurements in the transmission line. The radiated signals in far field regions are collected by the horn antenna with known gain to record the AUT radiation pattern with 3 D rotational traces using the 3 D positioning system, driven by the main control computer. Frequency down converters are used to process and analyse terahertz signals received by the horn, using VNA [33].

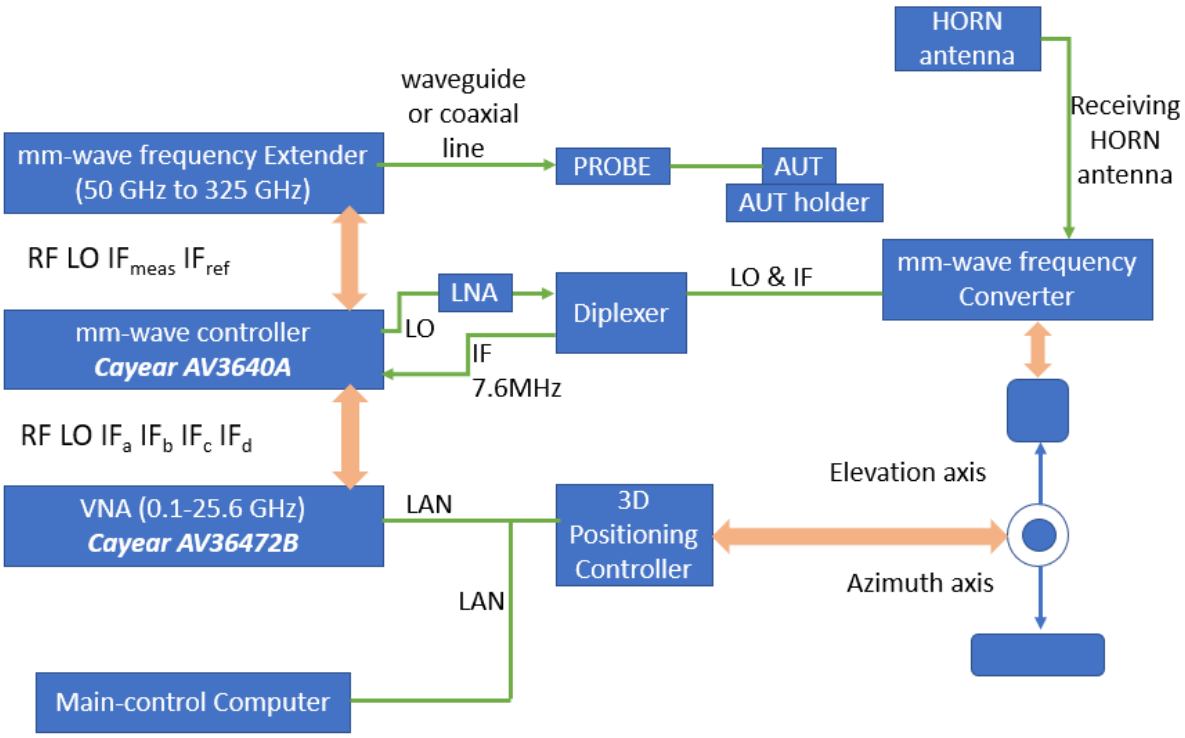

Figure 3. Terahertz frequency antenna measurement system [33].

AUT impedance measurement is calibrated as a first step, to obtain maximum performance of AUT in the system. The setup is limited for impedance measurements of single port only for this single port short-open-load (SOL) method of calibration is deployed. Probe feeding the transmission line either waveguide or coaxial cable is SOL tested and calibrated with impedance matching substrate (ISS) provided by manufacturer. Same is applied on chosen transmission line, waveguide or coaxial cable. Calibrated transmission line provides return loss measurements using VNA while feeding the AUT. Radiation pattern measurements are made by fixing probes and AUT in transmitter position. The horn antenna working as receiver, mounted on 3 D positioning system is rotated in 3 D trajectory using 3 D positioning controller. The horn feed the received signals to VNA for radiation pattern measurement. The trajectory instructions are made by the main control computer and feed to the positioning system and VNA. The VNA records the S_{21} parameters of the AUT radiation pattern at different test points in 3 D axis and plots the gain pattern [33].

5.3 Near Field Antenna System

The presented reconfigurable beam measurement system in figure 4 for optical astronomy can be considered for deployment in wireless communication system. The variable receiver system design in optical astronomy for beam measurements at frequencies with minor differences is taken as a problem and a reconfigurable beam measurement system is designed and tested at 0.9 THz and 1.37 THz with two different configurations. The measurement setup for 1.37 THz measurements is conducted at room temperature and is reviewed for deployment in wireless communication system. At 0.9 THz, the system is operating at cryogenic temperature can be best suited for optical astronomic measurements [34].

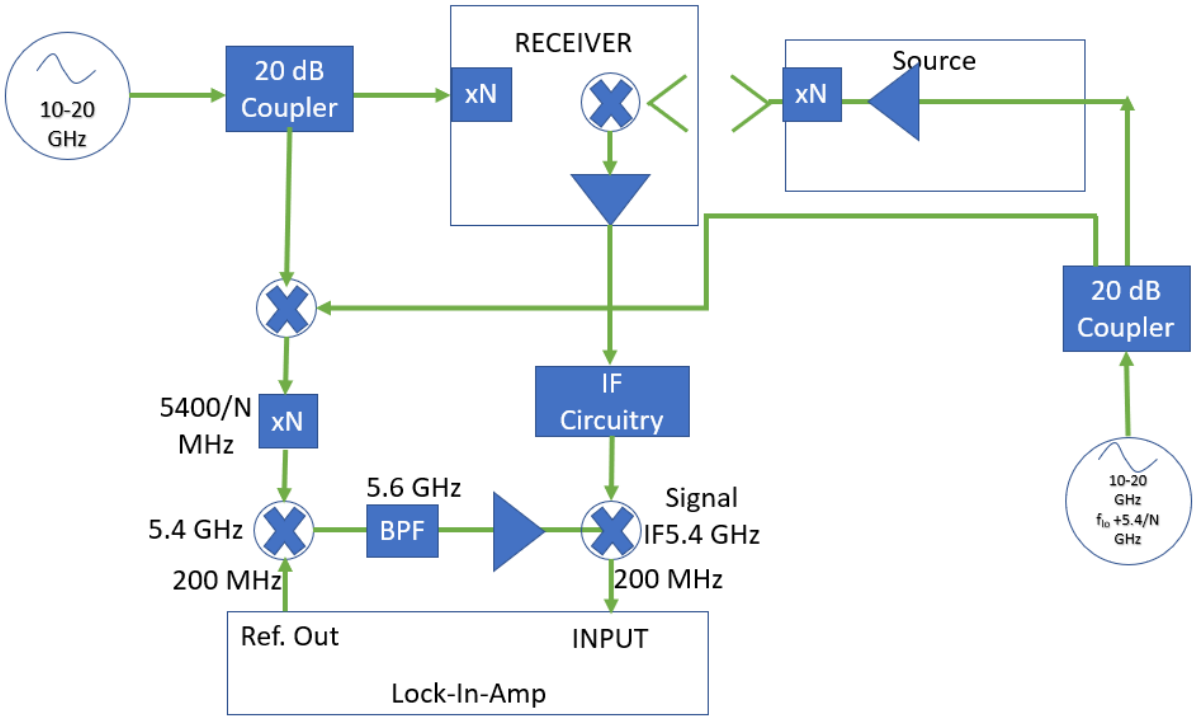

Figure 4. Block diagram of reconfigurable beam measurement system [34].

Measurement system design setup contains the waveguide guided horn connected to the RF sources via RF probe, which generates the beam pattern. A schottky diode is deployed as a receiver at room temperature for amplitude and phase measurements at 1.37 THz frequency. For 0.9 THz full astronomical receiver is deployed. The system is design to achieve beam pattern measurements for long frequency ranges with replacement of RF source and receiver to desired frequency and change of required microwave component in the setup. This leads to no major change in system setup and is considered as reconfiguration corresponding to frequency range to be tested. In the setup presented in figure 5, the couplers at receiver and source, take samples from the LO signal generator and RF signal generator [34].

The couplers feed the multiplexer with the LO and RF samples with a difference of 5.4/N GHz as an example. The mixer signal is down converted by a factor N; here N is the multiplier multiplication factor in RF and LO signal generator multipliers. In the next stage, the IF signal and reference signal from the downconverter is same in phase and frequency 5.4 GHz in the example. The IF signal is further down converted and is used as input to lock-in-amplifier. The multiplication factor N determines the operational RF frequency band in the system. The multiplications are done in steps using frequency doubler and tippler as presented in figure 5

for frequency extender, and figure 6 for low frequency reference signal generator. The presented frequency doubler and tippler are modified based on required RF frequency band measurements [34].

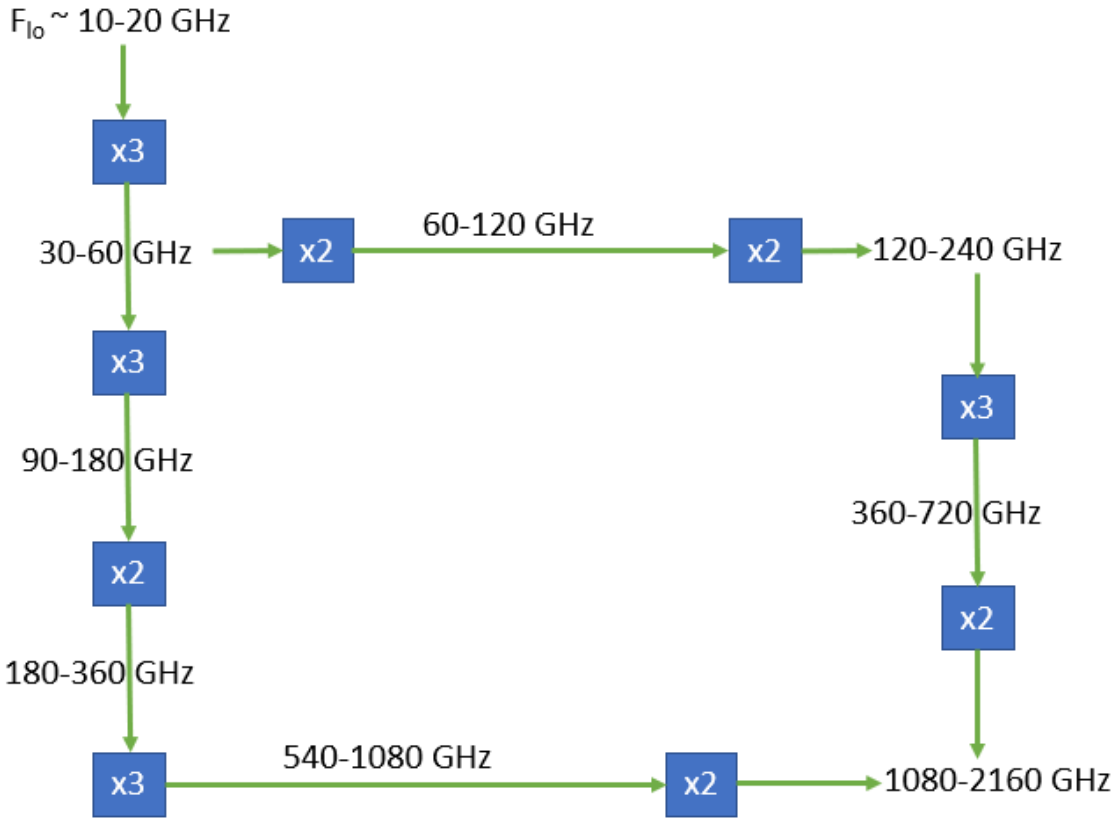

Figure 5. Frequency extender with multiple frequency doubler and tippler [34].

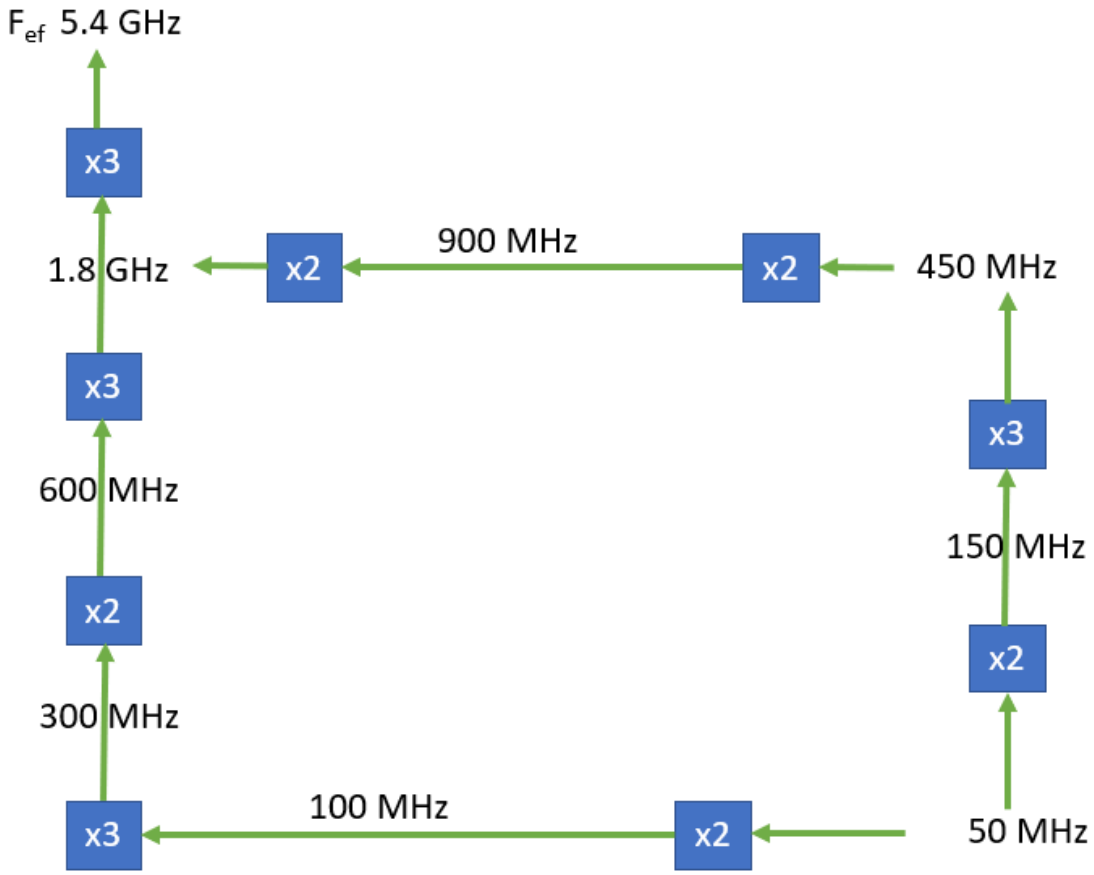

Figure 6. Low frequency reference signal generator with F_{ef} [34].

Room temperature measurements at 1.37 THz frequency range is obtained with direct multiplication of *N* (equals 108). A custom made Schottky diode is used as RF source. The probe horn is used at source for beam formation. For probe horn calibration, initially another prob horn with equivalent characteristics is used at receiver end. The receiver is fixed and RF source is placed on 4 axis positioning system. On the work bench receiver and RF source are placed in front of each other. The RF source follows a trajectory around the receiver via computer aid application lab view. Phase and amplitude beam measurements are recorded in co and crossed polarization. The results obtained at 1.37 THz are well detailed and plotted nicely, exhibits minor asymmetry due to fabrication material and assembly errors. This supports the stability of the measurement system. Long drifts in amplitude and phase measurements are contributions of active devices thermal instability and also dependent upon the RF band being measured with its reluctance towards environmental effects [34].

6 TERAHERTZ PROPAGATION MEASUREMENT SYSTEM

Study of radio wave propagation in any medium is crucial to design channel models for radio frequency band, which support in design and development of wireless communication techniques and equipment's, in wide range of radio frequency spectrum. With evolution of 5th generation of mobile communication, increased data rate demands and shortening of RF bandwidth, is exploring, extension in frequency band with widening of RF bandwidth, and bringing terahertz frequency spectrum into account for the future 6th and 7th generation of mobile communication. Propagation system designed for gigahertz spectrum is accounted and new propagation system and channel modelling is developed for terahertz frequency band system. In this thesis, we have done literature review of the existing research and designed system channel model for performance evolution in THz frequency band system are presented [27], [35].

In the design and development of any system model or communication technique, impulse response study of the system is vital. The channel model and propagation system of terahertz frequency band system for wireless communication, are modelled with system impulse response [27], [35].

6.1 Wideband Indoor System

The setup is bifurcated in two parts, one with the VNA of anritsu with model number MS4647B and other is virginia diodes inc (VDI) mixers modules with model number WR2.8MixAMC. The VNA has upper frequency limit of 70 GHz and is connected to the VDI mixer to upconvert the frequency for transmission [36]. VDI mixers modules contain the subharmonic mixers and perform frequency up conversion for transmission. After signal transmission from terahertz channel, the frequency is downconverter at receiver end for VNA recordings. The channel is characterized based on the transmitted and received signals at the VNA end [36].

VDI WR2.8MixAMC module operates at 260 GHz to 400 GHz at bandwidth of 20 GHz and with 15 dB loss during mixing. Yttrium iron garnet (YIG) based tunable synthesizer is used for stringent stability. The synthesizer generates LO frequencies from 10.79 GHz to 15.875 GHz. LO signal reaches VDI mixer via two frequency multiplexing stages [36]. At first stage LO get doubled (multiplied by 2) and afterwards the multiplied LO signal is feed to the multiply by 12 frequency multiplier and generates 260 GHz to 400 GHz. The complete setup is presented in the figure 7. The VDI mixers are connected to the transmitting and receiving horn antennas. S-parameter measurements are recorded using VNA [36].

Measurement setup calibration involves calibration of test instruments, VNA in this case. Error correction and calibrations are performed with interconnection of the Tx and Rx waveguide for optimal performance. The measurements are further taken using diagonal antennas at both ends. The antenna used are with gain of 25 dBi at centre frequency. Measurements are recorded at 10 points for full 19 GHz band measurements. Table 4 presents the measurement setup parameter configurations [36].

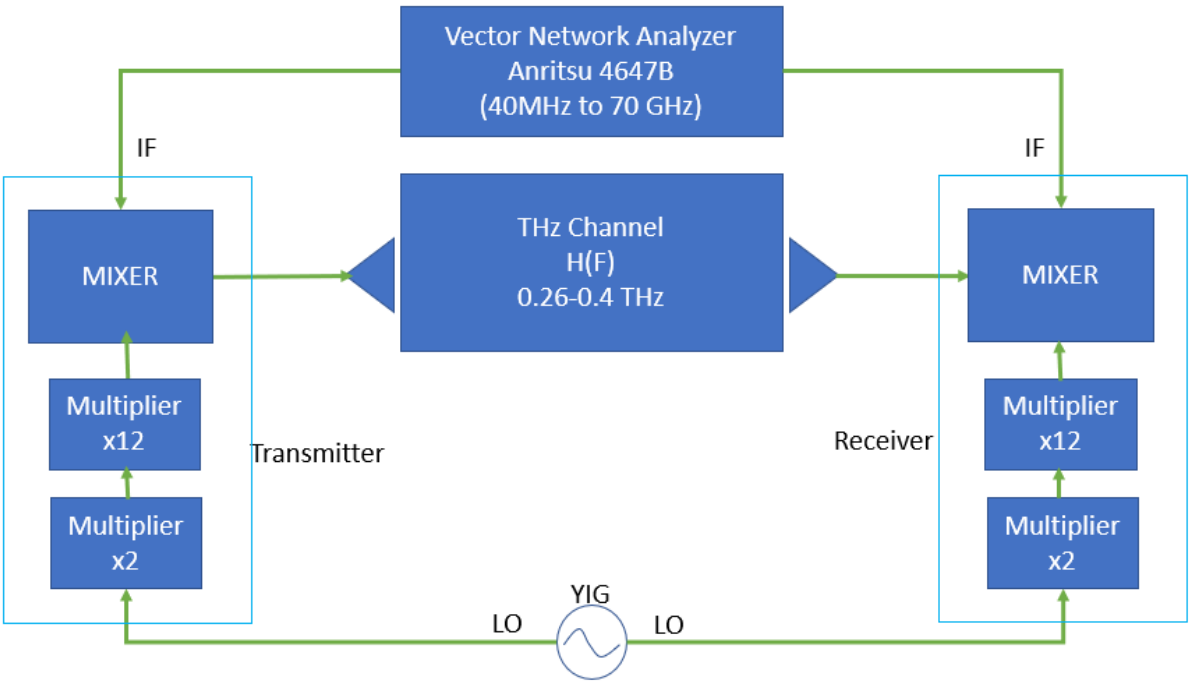

Figure 7. Wideband system block diagram [36].

Table 4. Measurement setup parameters [36].

Parameters	Values
Measurements Points	1000
Test Signal power	0 dBm
Start frequency	1 GHz
Stop Frequency	20 GHz
IF Bandwidth	1 KHz

The setup presented in figure 7 is for LoS measurement where measurement of transmission coefficient at different distances from 10 cm to 95 cm are recorded. Path loss measurements are conducted in 19 GHz segments and compiled to produce 260 GHz to 400 GHz frequency response. Measurement analysis shows increase in path loss with increase in distance, but the path loss response against the full spectrum for all the distance is similar [36]. The average path loss calculated for separation of 10 cm, 35 cm, 95 cm for frequency range of 260 GHz to 400 GHz is 14.23 dB, 24.14 dB and 35.75 dB respectively. This corresponds to the channel capacity of 9.26 b/s/Hz, 7.62 b/s/Hz, and 5.713 b/s/Hz. This leads to the fundamental of achieving 1.29 tbps at 140 GHz and is 200 times faster than current communication at distance of 10 cm [36].

NLoS measurements are taken at 35 cm separation by changing the angle of arrival by 0 degree to 30 degree in azimuth direction. The deployed highly directional antennas cause signal power drops and compensated using beamforming algorithm for viable tbps communications [36]. Shadowing in indoor environment causing heavy signal attenuations due to the presence of obstacles in between transmission paths is modelled. Shadowing due to human hand, glass of water, 80 grams of fiber material with thickness of 3 mm are measured in terms of signal attenuation as 45.6 dB, 6.14 dB and 27.55 dB at 290 GHz frequency [36].

The NLoS and LoS link capacity measurements are conducted at different Tx-Rx separations and at different angle of arrival and are presented in the table below.

Table 5. LOS and NLOS links capacity comparison [36].

LINK	Tx & Rx separation (cm)	Observation	Angle of arrival (degree)	Capacity (b/s/Hz)
LOS	10	-	-	9.26
	35	-	-	7.26
	95	-	-	5.713
NLOS	35	-	5	7.03
	35	-	10	6.44
	35	-	30	3.23
	35	Fiber material	-	6.732
	10	Ceiling panel	90	6.719

6.2 VNA Based System

A custom configurable channel sounder is deployed, to control signal with smaller wavelengths under terahertz range attenuation. The testbed contains the frequency domain setup for wideband channel characterization. In instrumentation, a VNA of keysight technologies with model number N52478 is connected to the frequency extender of virginia diode inc (VDI) with operating range of 140 GHz to 220 GHz. The VNA feeds IF frequency of 0.01 GHz to 67 GHz to VDI extenders. The setup is presented in figure 8, here frequency extenders are feed with LO (local oscillator) signals with frequency range 11.67 GHz to 18.33 GHz [37].

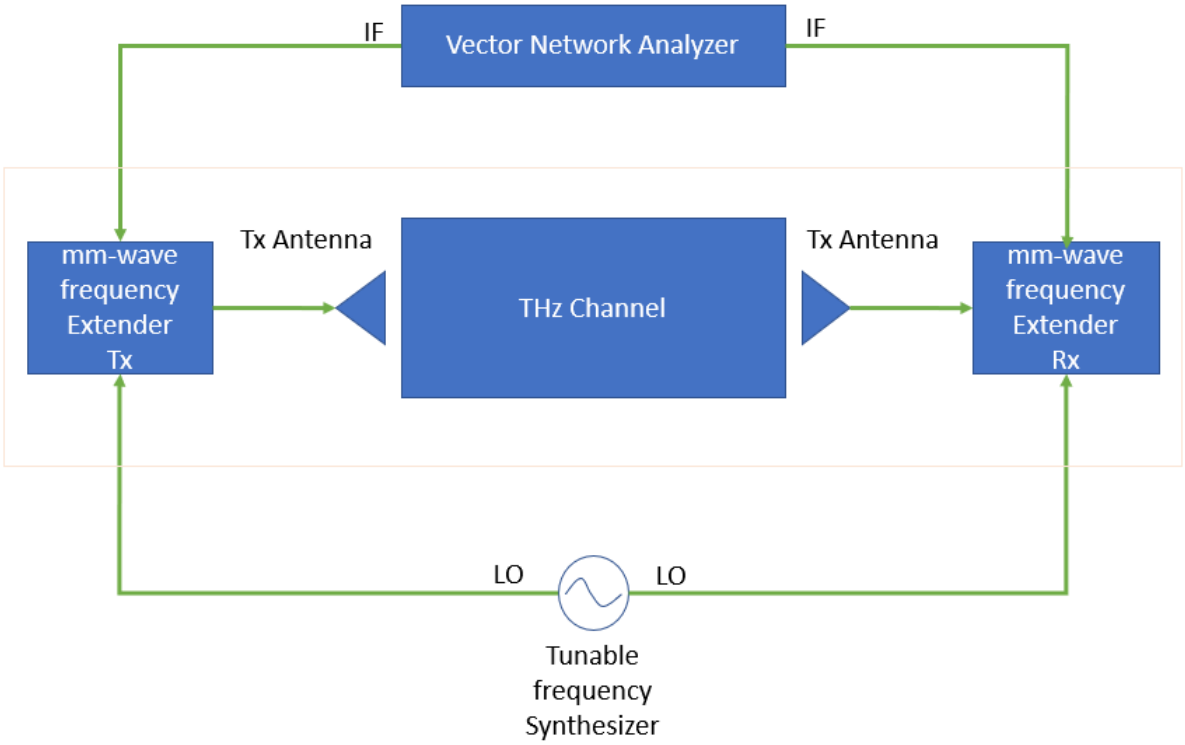

Figure 8. VNA based measurement block diagram [37].

LO signals are generated by frequency synthesizer and extended to desired range in terahertz by multiplication of 12 with use of VDI extenders. The VDI extenders are connected to the directional horn antennas at transmitter and receiver and are aligned in LoS positions on work bead. Transmitter antenna radiates sounding signal of mixed IF and multiplied LO in line of sight direction to the receiver. Received signal down conversion takes place at the receiver end. The setup before measurements is calibrated using VDI calibration kit [37].

The measurements are conducted in indoor environment with architectural consideration as office environment, involving desk, chairs and other usual materials. LoS positioning and separations are carried out using laser crosshair and pointers to obtain high level precision. The below figure 9 presents the Tx and different Rx positions. Rx movements are carried out from 0.5 m to 5.5 m [37].

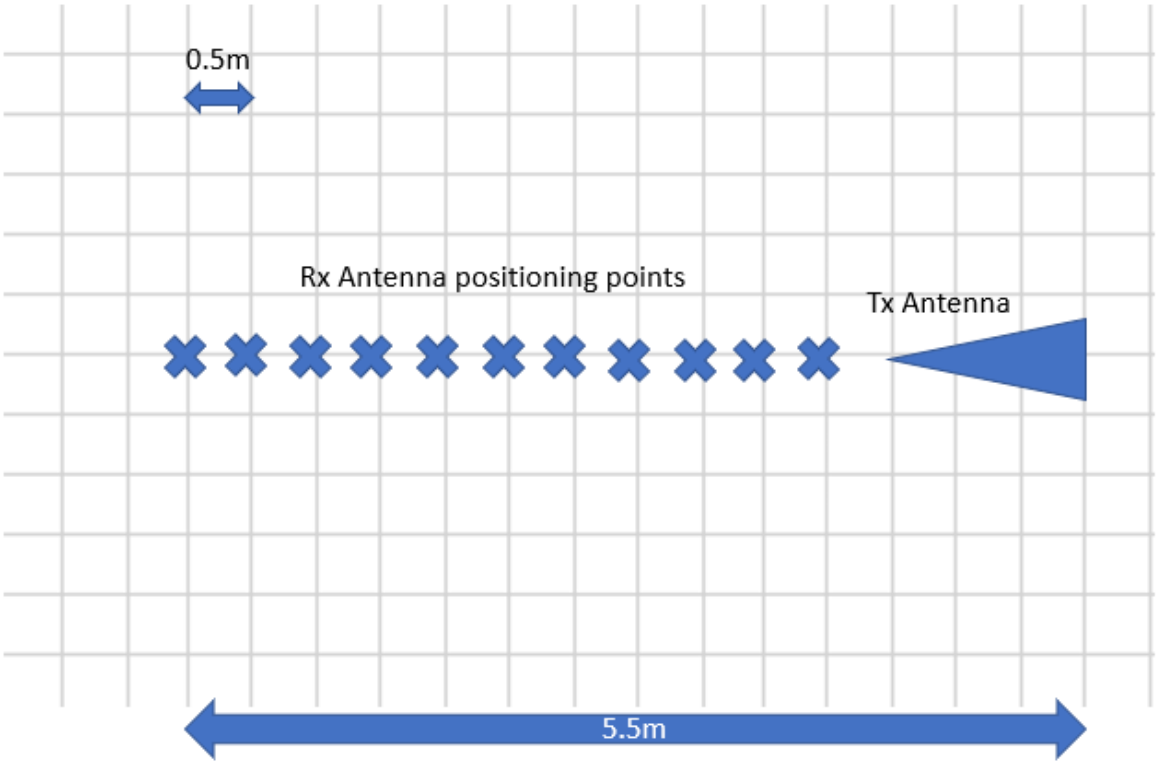

Figure 9. Tx-Rx mapping [37].

Table 6 below presents the key measurement setup parameters. Based on it, setup measurement limits are calculated as having 16 MHz frequency resolution, 0.0625 microseconds of excessive delay and 18.75 m of excessive distance, a multipath can travel to be detected [37].

Table 6. Measurement setup parameters [37].

Parameters	Values
Measurements Points	5000
Averaging factor	10
Start frequency	0.14 THz
Stop Frequency	0.22 THz
THz, IF	279 MHz

The LoS measurements at different Tx-Rx separations, presents path loss increments with log of distance. Similar variations in path loss, across the band are recorded over all separation values. PDP measurements are conducted at different separation points and are analyzed for 0.5 m, 1.5 m, 2.5 m, 3.5 m, 4.5 m, 5.5 m Tx/Rx separation points, stated in figure 9 as well. Major multipath components are recorded at 0.5 m only and states higher directivity of terahertz signals [37]. Future work is proposed for both indoor and outdoor MIMO scenarios.

6.3 Ultra Wideband Indoor System

Measurement system for channel characterization and modelling for Terahertz frequency band of 0.5 THz to 0.75 THz with bandwidth of 0.25 THz is reviewed for setup deployment, terahertz instrumentation, measurement setup calibration and power delay profile (PDP) measurements. The channel carried out LoS propagation of the signals in indoor environment. The measurements are taken at different iterations of receiver antenna positions and channel impulse response is recorded and presented for power delay profile analysis. Multiple delays are recorded at reflections points, due to work bench and group delay products [38].

The setup contains transmitter and receiver arranged in LoS configuration, using positioners attached to the workbench. A VNA of keysight technologies with model number PNA-X. The VNA is attached to two vector network analyzer extender of virginia diodes inc (VDI) and is configured for them. Both VDI extenders heads are fitted with WM-380 waveguide ports. The VDI extender heads are tuned to 500 GHz to 750 GHz and are attached to diagonal horns. The setup is presented in figure 10. S-parameter measurements are recorded from the workbench setup and are further extended for PDP analysis, considering the atmospheric effect, causing multipath propagations and molecular absorptions [38].

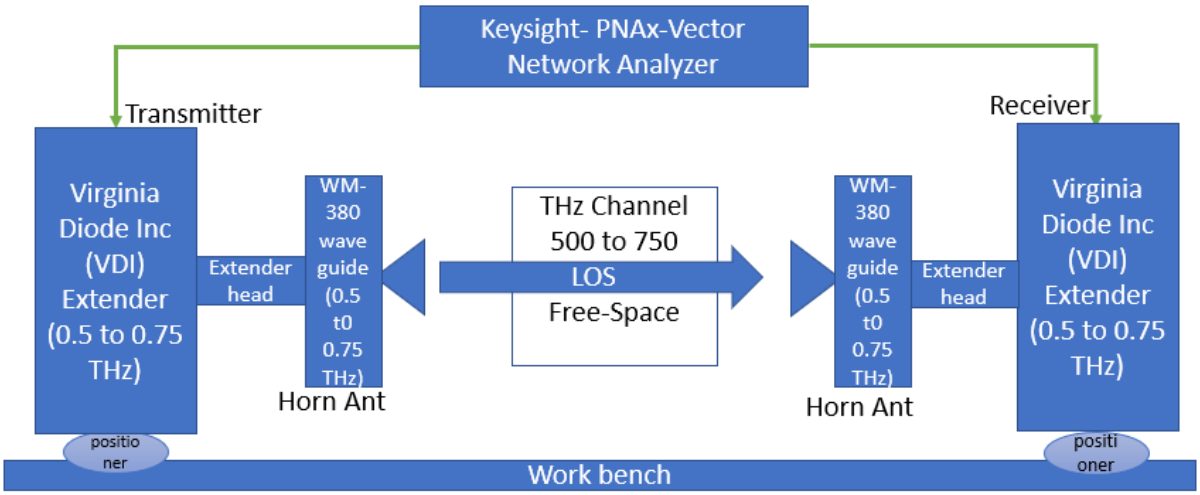

Figure 10. Ultra wideband block diagram [38].

Short, offset-short, load and thru (SOLT) technique is used for VDI extender heads calibration. The short, offset-short, load as one port devices defines reflection standards and are used together with thru (2 port device) for transmission measurement corrections, containing load matching, transmission tracking, crosstalk errors. The calibrated extender heads are then attached to the diagonal horns and positioned on workbench in LoS positioning for s parameter measurements [38].

Considering the absorption of EM waves by atmospheric oxygen and water molecules during free space propagation, including other effects as pressure, temperature, and humidity. The channel model for free space terahertz propagation is created for atmospheric attenuation. The measurements carried out has shown higher level of attenuation at 557 GHz and 750 GHz [38].

Power delay profile (PDP) measurements are recorded for analysis of atmospheric attenuations and major dip in PDP intensity points corresponding to frequency band from 500 GHz to 750 GHz are analyzed. At frequency level of 557 GHz a major dip in PDP intensity is recorded, due to atmospheric molecular absorption due to oxygen and water. Attenuation recorded at 750 GHz on the boundary is not observable, being last frequency point; measurement setup is under limit of 750 GHz. The measurements present decrease in signal strength with increase in frequency. Due to setup limitations, the decrease in atmospheric effect after 750 GHz are not recorded and are normalized [38].

1600 data points are recorded for received power at various antenna separations with delay resolution of 0.004 ns. The small delay resolution resolves multipath effects. Repetition of received power profile at 0,2,4, inch separations are seen in rest measurements [38]. In the same way, PDP peaks for thru and largest separation (0 inches and 9 inches) are analyzed and corresponding LOS and group delay components are recorded. LOS component is observed at 0 ns and 0.76 ns for 0 inches and 9 inches separations. The group delay component is observed at relative delay of 0.52 ns at 9 inches separation. The other delays are considered to be due to reflections caused by work bench and in overall analysis molecular absorption effect on measured PDP waveforms is considerably low and non-significant [38].

7 DISCUSSION

Terahertz antenna parameters presented in the chapter 3 are taken as standard to review and report the terahertz antenna measurement system and techniques are presented in chapter 5. The measurement system reported in sub chapter 5.1 for measurement of terahertz antenna gain, radiation pattern in 2 D and 3 D models in frequency range of 220 GHz to 330 GHz has certain limitation in workbench setup. The designed coordinate system working as a positioner in the setup is limited in azimuth angle from 0 degree to 180 degree, which limits the radiation pattern measurements. The limitation is conquered with use of external mechanical extenders. The reconfigurable terahertz antenna measurement system reported in sub chapter 5.3 is tremendously good for beam pattern measurements for 0.03 THz to 1.6 THz range. The system advantage works on antenna parameter measurements for a wide range of terahertz frequency band and need insignificant changes in the work bench setup, procedure and instrumentation.

Terahertz wave propagation parameters are presented in chapter 4. The relative measurement systems are reported in chapter 6. Sub chapter 6.1 reported measurement system for LOS and NLOS link in 260 GHz to 400 GHz. The study is carried out in contrast of use of the terahertz frequency range for 5G and above wireless and mobile communication system. The measurements of path loss, reflection, shadowing has validated the system setup and procedure. The measurement of channel capacity in terabits per second for LOS and NLOS link supported its use in wireless and mobile communication system. The measurement system presented in sub chapter 6.3 has limitation to carry out measurement in short range distance only, because of low signal power at receiver level. The presented limitations of the setup is considered to be non impacting for realistic measurements in indoor environment. The terahertz propagation measurement system presented in sub chapter 6.1 is considered. Which are good for use in wireless communication development and the associated advantage is calculation of channel capacity and data rates in both LOS and NLOS links.

8 SUMMARY

In this thesis, literature review of different methods and techniques in terahertz antenna measurement system and terahertz wave propagation measurement system are reported for their use in wireless communication system. The study presented in the thesis begins with the findings of terahertz frequency band range and application in wireless communication system in chapter 2. The study is further extended for detailed understanding of terahertz antenna and terahertz wave propagation parameters in chapter 3 and chapter 4, and a complete review of available setups, methods and procedures for measuring these parameters in chapter 5 and chapter 6.

Chapter 2 reported the allocation of terahertz frequency range from 100 GHz to 3 THz, in the available radio frequency spectrum. Terahertz frequency channel segregation and standardization by FCC, ITU, ETSI is presented and allocated frequency range to carry out research for wireless applications is reported in the sub chapter 2.1.1. Terahertz frequency application in wireless communication and for other use are tabularized in sub chapter 2.2.

Terahertz antenna parameters are reported in chapter 3 with detailed understanding to further extend the study for review of terahertz antenna measurement system methods and techniques. The parameters presented are radiation pattern, beamwidth, directivity, efficiency, gain and bandwidth.

In chapter 4, study of terahertz propagation, with the plane wave model in different medium and terahertz channel modelling is reported. The study presented propagation of plane wave, through different medium, comprises of lossless media, lossy media, lossless media boundaries, lossy media boundaries, rough surface and diffracted edges in chapter 4.1. The propagation parameters including path loss, shadowing, fading, channel noise, frequency and impulse response, are reported in chapter 4.2 using channel modelling studies.

Available terahertz antenna measurement systems are reported in chapter 5. Including measurement system with custom build spherical positioning system reported in sub chapter 5.1 for measurement of s-parameters in antenna far field region under 220GHz and 330GHz frequency range. Another measurement technique reported in sub chapter 5.2 measures antenna impedance and radiation pattern in antenna far field region under 325 GHz frequency range. Sub chapter 5.3 presents reconfigurable beam measurement setup with the ability to carry out measurements under wide terahertz frequency range with minimal changes in the setup. The setup is tested for received power amplitude and antenna radiation pattern measurements at 1.37 THz.

Terahertz wave propagation measurement systems with associated setups and procedures are reported in chapter 6. Sub chapter 6.1 presents the literature review of measurement setup for LOS and NLOS propagation measurements under 270 to 400 GHz. Path loss measurements were taken for both the LOS and NLOS links and based on it, data-rate capacity comparisons are made for application in 5G wireless communication system. Measurement system for indoor channel LOS propagation for PDP measurements is reviewed in sub chapter 6.2. The measurements are conducted in indoor environment with architectural consideration as office environment, involving desk, chairs and other usual material for real world wireless applications. In sub chapter 6.3, measurement technique for channel characterization of terahertz frequency band 0.5 THz to 0.75 THz is reviewed. Channel impulse response and PDP measurements are conducted for study of effect of molecular absorptions due to presence of oxygen and water molecules in the air.

9 REFERENCES

[1] S. Supervisor, T. Advisor, and S. Rahaman, "MASTER ' S THESIS Comparative Study of Increasing Indoor WLAN Coverage by Passive Repeating Systems," no. May, 2018.

[2] B. Khani, S. Makhlouf, A. G. Steffan, J. Honecker, and A. Stohr, "Planar 0.05-1.1 THz laminate-based transition designs for integrating high-frequency photodiodes with rectangular waveguides," *J. Light. Technol.*, vol. 37, no. 3, pp. 1037–1044, 2019.

[3] H. Yi, K. Guan, D. He, B. Ai, J. Dou, and J. Kim, "Characterization for the Vehicle-to-Infrastructure Channel in Urban and Highway Scenarios at the Terahertz Band," *IEEE Access*, vol. 7, pp. 166984–166996, 2019.

[4] L. Pometcu and R. D'Errico, "An indoor channel model for high data-rate communications in D-band," *IEEE Access*, vol. 8, pp. 9420–9433, 2020.

[5] A. Regmi, "Reflection Measurement of Building Materials At Microwaves," 2016.

[6] M. Mimo and B. Station, "MASTER ' S THESIS BEHAVIOR OF THE RF POWER AMPLIFIER UNDER A VARYING LOAD CONDITION IN 5G," no. August, 2018.

[7] S. Examiner, T. Advisor, M. Y. Javed, A. Parssinen, T. Rahkonen, and N. Tervo, "MASTER ' S THESIS CHARACTERIZING NONLINEARITY IN," no. November, 2017.

[8] M. Berg, "Master ' S Thesis Simplifying the Radiation Pattern Modeling and Considering the Mutual Coupling in Linear Dipole Antenna," no. February, 2018.

[9] Y. Huo, X. Dong, W. Xu, and M. Yuen, "Enabling Multi-Functional 5G and beyond User Equipment: A Survey and Tutorial," *IEEE Access*, vol. 7, pp. 116975–117008, 2019.

[10] J. Sun and S. Lucyszyn, "Extracting Complex Dielectric Properties from Reflection-Transmission Mode Spectroscopy," *IEEE Access*, vol. 6, pp. 8302–8321, 2018.

[11] M. Pigeon *et al.*, "From simulations to measurements: Prototyping an antenna for non-linear applications at sub-THz frequencies," *IET Microwaves, Antennas Propag.*, vol. 11, no. 3, pp. 304–309, 2017.

[12] C. Ciano *et al.*, "Confocal Imaging at 0.3 THz with Depth Resolution of a Painted Wood Artwork for the Identification of Buried Thin Metal Foils," *IEEE Trans. Terahertz Sci. Technol.*, vol. 8, no. 4, pp. 390–396, 2018.

[13] K. Guo, A. Standaert, and P. Reynaert, "A 525-556-GHz Radiating Source With a Dielectric Lens Antenna in 28-nm CMOS," *IEEE Trans. Terahertz Sci. Technol.*, vol. 8, no. 3, pp. 340–349, 2018.

[14] J. Grajal *et al.*, "Compact Radar Front-End for an Imaging Radar at 300 GHz," *IEEE Trans. Terahertz Sci. Technol.*, vol. 7, no. 3, pp. 268–273, 2017.

[15] Binbin Cheng *et al.*, "Real-Time Imaging With a 140 GHz Inverse Synthetic Aperture Radar," *IEEE Trans. Terahertz Sci. Technol.*, vol. 3, no. 5, pp. 594–605, 2013.

[16] Y. R. Huang *et al.*, "Propagation, resonance, and radiation on terahertz optoelectronic integrated circuits," *IEEE Photonics J.*, vol. 4, no. 3, pp. 699–706, 2012.

[17] T. S. Rappaport *et al.*, "Wireless communications and applications above 100 GHz: Opportunities and challenges for 6g and beyond," *IEEE Access*, vol. 7, pp. 78729–78757, 2019.

[18] Jones, G., Layer, D., & Osenkowsky, T. (2007). National Association of Broadcasters Engineering Handbook: NAB Engineering Handbook (E. Williams, Ed.) (10th ed.). Routledge. https://doi.org/10.4324/9780080927282.

[19] H. Elayan, O. Amin, B. Shihada, R. M. Shubair, and M. S. Alouini, “Terahertz band: The last piece of rf spectrum puzzle for communication systems,” *arXiv*, vol. 1, no. October 2019, pp. 1–32, 2019.

[20] D. No, “This document is being released as part of a ‘permit-but-disclose’ proceeding. Any presentations or views on the subject expressed to the Commission or its staff, including by email, must be filed in ET Docket No. 18-21, which may be accessed via the Elec,” no. 18, 2018.

[21] L. Cang, H. K. Zhao, and G. X. Zheng, “The Impact of Atmospheric Turbulence on Terahertz Communication,” *IEEE Access*, vol. 7, pp. 88685–88692, 2019.

[22] T. Komine and M. Nakagawa, "Fundamental analysis for visible-light communication system using LED lights," in IEEE Transactions on Consumer Electronics, vol. 50, no. 1, pp. 100-107, Feb. 2004, doi: 10.1109/TCE.2004.1277847.

[23] Y. Niu, Y. Li, D. Jin, L. Su, and A. V. Vasilakos, “A survey of millimeter wave communications (mmWave) for 5G: opportunities and challenges,” *Wirel. Networks*, vol. 21, no. 8, pp. 2657–2676, 2015.

[24] S. Abadal, C. Han, and J. M. Jornet, “Wave Propagation and Channel Modeling in Chip-Scale Wireless Communications: A Survey from Millimeter-Wave to Terahertz and Optics,” *IEEE Access*, vol. 8, pp. 278–293, 2020.

[25] Rambo, S. (2018, April 18). FCC opens comment on two 5G mmWave spectrum auctions. Retrieved from U.S. 5G spectrum auctions for 24, 28 GHz bands set to begin in November.: https://www.rcrwireless.com/20180418/5g/fcc_opens_comment_5g_mmwave_spectrum.

[26] N. Grace, “FCC Proposes More Spectrum for Unlicensed Use,” *Compliance Eng.*, vol. 20, no. 4, pp. 12–14, 2003.

[27] Saunders SR, Aragón-Zavala A. Antennas and propagation for wireless communication systems. 2nd ed ed. Chichester: Wiley; 2007:xxii, 524 sivua. https://oula.finna.fi/Record/oy.999588593906252.

[28] S. A. Sahdman, K. S. Islam, S. S. Ahmed, S. S. Siddiqui and F. Shabnam, "Comparison of Antenna Parameters for Different Substrate Materials at Terahertz Frequency Region," 2019 IEEE 5th International Conference on Computer and Communications (ICCC), Chengdu, China, 2019, pp. 680-684, doi: 10.1109/ICCC47050.2019.9064424.

[29] Y. He, Y. Chen, L. Zhang, S. Wong and Z. N. Chen, "An overview of terahertz antennas," in China Communications, vol. 17, no. 7, pp. 124-165, July 2020, doi: 10.23919/J.CC.2020.07.011.

[30] Balanis CA. Antenna theory : Analysis and design. Fourth edition ed. Hoboken: John Wiley;2016:1verkkoaineisto. https://oula.finna.fi/Record/oy_electronic_oy.9916176513906252.

[31] N. Chudpooti, N. Duangrit, P. Akkaraekthalin, I. D. Robertson, and N. Somjit, “Electronics-based free-space terahertz measurement using hemispherical lens antennas,” *IEEE Access*, vol. 7, pp. 95536–95546, 2019.

[32] B. Sievert, J. T. Svejda, D. Erni and A. Rennings, "Spherical mm-Wave/THz Antenna Measurement System," in IEEE Access, vol. 8, pp. 89680-89691, 2020, doi: 10.1109/ACCESS.2020.2993698.

[33] Z. Zheng, Y. Zhang and J. Mao, "Testing Method of a Millimeter-Wave/THz Far-Field Antenna Measurement Setup," 2020 9th Asia-Pacific Conference on Antennas and Propagation (APCAP), 2020, pp. 1-2, doi: 10.1109/APCAP50217.2020.9246020.

[34] A. Gonzalez, Y. Fujii, T. Kojima and S. Asayama, "Reconfigurable Near-Field Beam Pattern Measurement System From 0.03 to 1.6 THz," in IEEE Transactions on Terahertz Science and Technology, vol. 6, no. 2, pp. 300-305, March 2016, doi: 10.1109/TTHZ.2016.2526643.

[35] E. N. Papasotiriou, J. Kokkoniemi, A. A. A. Boulogeorgos, J. Lehtomaki, A. Alexiou, and M. Juntti, “A new look to 275 to 400 GHz band: Channel model and performance evaluation,” *IEEE Int. Symp. Pers. Indoor Mob. Radio Commun. PIMRC*, vol. 2018-September, pp. 1–5, 2018.

[36] N. Khalid and O. B. Akan, "Wideband THz communication channel measurements for 5G indoor wireless networks," 2016 IEEE International Conference on Communications (ICC), Kuala Lumpur, Malaysia, 2016, pp. 1-6, doi: 10.1109/ICC.2016.7511280.

[37] N. A. Abbasi, A. Hariharan, A. M. Nair and A. F. Molisch, "Channel Measurements and Path loss Modeling for Indoor THz Communication," 2020 14th European Conference on Antennas and Propagation (EuCAP), Copenhagen, Denmark, 2020, pp. 1-5, doi: 10.23919/EuCAP48036.2020.9135643.

[38] D. Serghiou et al., "Ultra-Wideband Terahertz Channel Propagation Measurements from 500 to 750 GHz," 2020 International Conference on UK-China Emerging Technologies (UCET), 2020, pp. 1-4, doi: 10.1109/UCET51115.2020.9205476.